



Preparation and Study of the Structural and Optical Properties of TiO₂ – Ag-ZnO Nanoparticles

Nooraluhda Zaid ^{*}, Tahseen H. Mubarak  and Nadia M. Jassim 

Department of Physics, College of Science, Diyala University

[*nooralhuda184@gmail.com](mailto:nooralhuda184@gmail.com)

This article is open-access under the CC BY 4.0 license(<http://creativecommons.org/licenses/by/4.0>)

Received: 5 February 2024

Accepted: 12 March 2024

Published: 30 April 2025

DOI: <https://dx.doi.org/10.24237/ASJ.03.02.850C>

Abstract

TiO₂, Ag, ZnO, TiO₂Ag NPs and TiO₂-Ag-ZnO NPs were prepared using pulsed laser ablation in liquids (PLAL) Technique. The effect of number of pulses (550, 650, 800) on the structural and optical properties of nanoparticles prepared in distilled water (DW) as growth media were examined using a Q-Switched Nd-YAG laser at wavelength (1064 nm) , ablation energy (610 mJ). As for the (Ag NPs, TiO₂ NPs, ZnO NPs, TiO₂-Ag and TiO₂-Ag-ZnO NPs) they were hybridized by the volumetric method. The results of (FE-SEM) for samples prepared with distilled water (DW) showed that the Particle size was (39.1, 62.4, 23.8 nm) for (Ag NPs) and the Particle size (34.26, 49.04, 32.1 nm) for (TiO₂ NPs), and the Particle size (36.54 , 37.86, 30.54 nm) for Zinc Oxide NPs, hybrid (TiO₂-Ag) nanoparticles was the Particle size nanoparticles (44.17, 33.73, 42.91 nm), and hybrid (TiO₂-Ag-ZnO) nanoparticles was the Particle size nanoparticles (53.58 , 45.15 nm). The FTIR results indicated that vibration coupling (Ag-O), (Ti-O), and the absorption beam appears the beam vibration (H-O), and that the absorption beam appearing near the wave number of vibration of Zn-O. The optical properties of (Ag NPs, TiO₂ NPs, ZnO NPs, TiO₂-Ag and TiO₂-Ag-ZnO NPs). The results in pulsed 800 of (UV-Vis) indicated a characteristic peak of range (199-200) and (403-411 nm) wavelength. On biological application, (Ag NPs, TiO₂ NPs, ZnO NPs, TiO₂-Ag and TiO₂-Ag-ZnO NPs) prepared with different laser standards in distilled water were used as anti-bacterial



agents. (*Staphylococcus aureus*, *Escherichia coli*, *Proteus mirabilis* and genus *Streptococcus*) indicated the highest bacterial inhibition in the hybrid $\text{TiO}_2\text{-Ag-ZnO}$.

Keywords: The Dioxide Titanium, pulsed laser ablation in liquids, Silver nanoparticules, Zinc Oxide

Introduction

In our modern society, the nanosciences have as of late developed as a noteworthy research course, resulting from continuous endeavours to make anything in a nanometer size using various tools and processes. Particularly in the nanoparticle synthesis [1].

Colloidal metal nanoparticles are of great interest for researchers from a wide range of disciplines including materials science, physics, engineering and chemistry due to its unique magnetic, electronic and optical properties [2, 3].

The nanoscale size causes electron confinement in metal nanoparticles resulting in the surface plasmon resonance (SPR) property. Metals nanoparticles exhibit improved properties such as plasmon resonance characteristics depending upon their size and morphologies [4].

Plasmons are density waves of the free outer electrons. Specific wavelengths of light cause the outer electrons to oscillate. This phenomenon is called the surface plasmon resonance (SPR). When these resonances occur, the intensities of absorption and scattering are much higher than those of the same particles without plasmonic properties. Surface plasmon resonance (SPR) are highly dependent on particle characteristics [5, 6].

A major challenge in nanotechnology is how to fabricate nanostructures with optimized figure-of-merit for different applications and from different materials.

Generally, there are two classes of approaches to fabricate nanostructures, namely, bottom-up assembly and top-down fabrication [7]. Laser ablation of solids is a top-down method, which has attracted much interest ever since the invention of ruby laser in 1960s [8,9], the generation of micro-nanostructures by laser ablation is usually a bottom-up process represented by nucleation, growth and assembly of clusters from laser ablated species.

Methods

1. Nanocrystalline colloidal solutions were prepared from the silver noble metals (Ag), and the non-noble metals titanium (TiO_2) and ZnO.



2. Then the hybrid material was prepared (TiO₂NPs, AgNPs, ZnONPs, TiO₂-AgNPs, TiO₂-Ag-ZnONPs).
3. The materials (TiO₂, Ag, Zn) used and the devices used to study the structural and optical properties of the nanoparticles were prepared by means of laser ablation pulses. For metallic targets with high purity 9.99% (silver and titanium and Zn), (Dw) (distilled water)
4. The system includes a laser source. (Q-Switched Nd: YAG) China originating from (HUAFEI) company in two wavelengths (1064, 532) nm. With maximum energy (1000) mJ per pulse (550, 650, 800) and pulse time (10) ns. Repetition rate (1) Hz and effective beam diameter (2) mm which is used for ablation. The lens used has a focal length of (20) cm to achieve high laser flux.
5. The removal of metal targets took place in the postgraduate laboratories of the Department of Physics, Faculty of Science, Diyala University, Iraq.

Target of Material

In this study, metallic targets of silver, and titanium were used they were purchased from the local market and are of high purity (9.99%) before starting an operation.

Preparation of Nanoparticles

1. The colloidal solutions of nanoparticles of minerals were prepared using high purity (9.99%) silver and titanium and zinc oxide targets, using the pulse laser ablation technique (PLAL) in liquid and at room temperature. As shown in Figure (1).
2. The metal targets were polished and cleaned before and after each eradication process by washing them with ethanol and then with distilled water using an ultrasound device (Ultrasonic path), and then cleaning the targets to get rid of the impurities.
3. Then the target was placed at the bottom of a glass container and submerged in distilled water (DW) and the volume of water used in all eradication operations was (3) ml and the height of the liquid above the target surface is (3) mm. In the current study, the number of laser pulses was changed as a function of the energies of each pulse.

4. The energy used is (610 mJ) per pulse. Where the number of laser pulses that bombed the surface of the metal targets were (550, 650, 800) pulses at a fixed laser energy of (610 mJ). In the present work, for every target utilized, there was a (7 cm) gap between the target and the laser lens .
5. The width of the laser beam on the superficial of the metallic target was 2 mm.
6. The targets were bombarded with a (Nd: YAG) laser of wavelength (1064) nm with a pulse time of (10) ns and a frequency of (1) Hz to obtain colored colloidal solutions containing the nanoparticles of the metal targets that were removed as the water changed color after the eradication process. Figure (1-2) shows the mechanism of action of the pulse laser ablation device

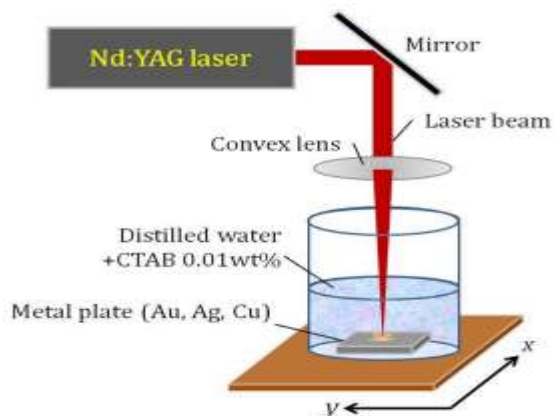


Figure 1: Setup of pulse laser ablation in liquid.

Results

X-Ray Diffraction

Figure (2) shows the XRD of Ag-TiO₂-ZnO nanoparticles. The results of the X-ray tests showed the presence of the three elements, according to the standard cards mentioned previously, the peaks at $2\theta=38.11$ and 44.5 characterize Ag foundations and the peak at $2\theta=22.6, 27.8$ and 44.5 characterize the animation of rutile TiO₂ and the peaks at $2\theta = 32.2, 32.9, 35.3$ and 46.2 represent the existence of rutile ZnO [104,105].

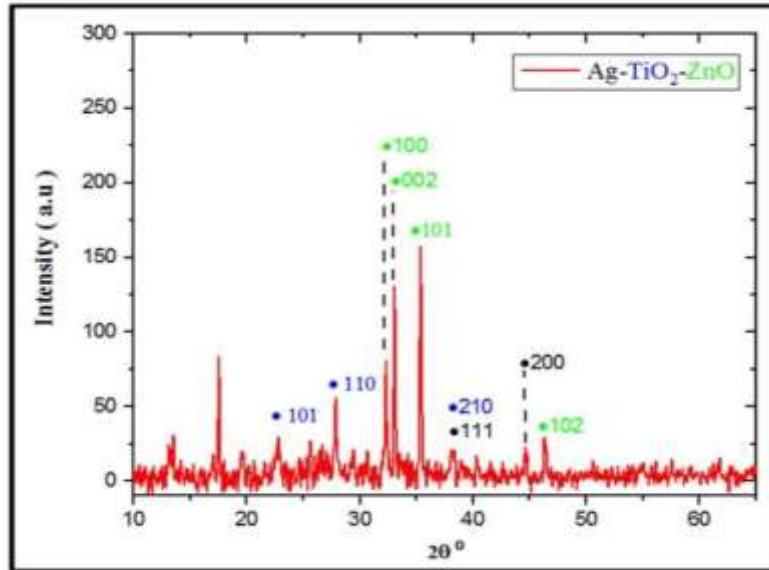
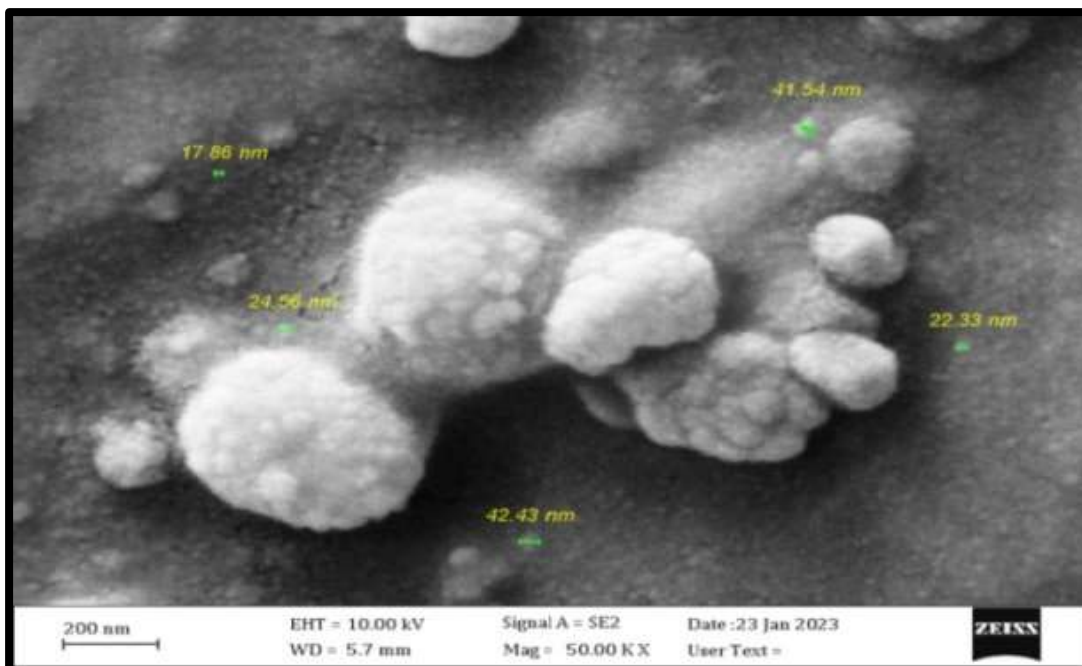
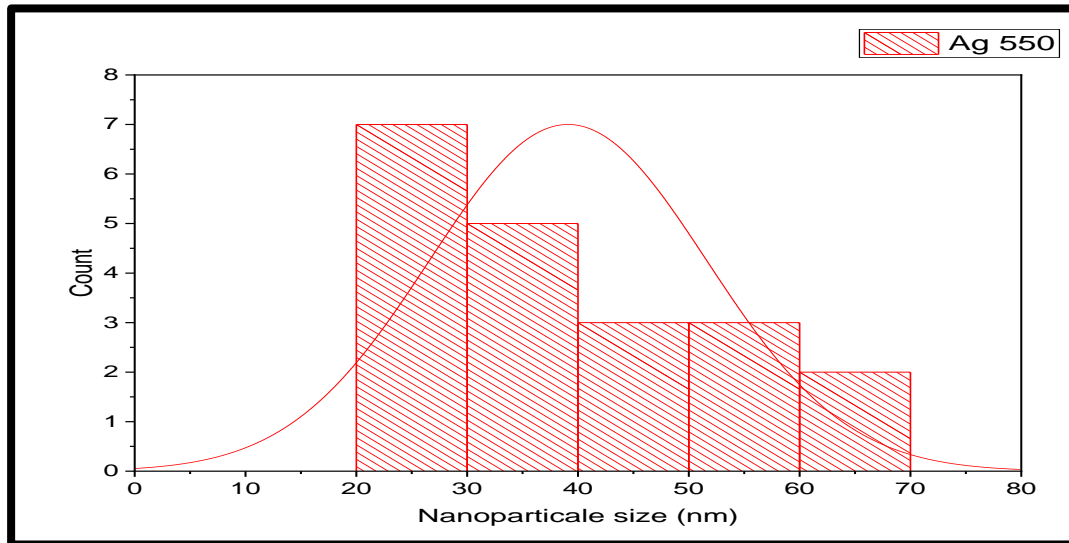


Figure 2: shows X-Ray Diffraction Ag-TiO₂ -ZnO

FE-SEM

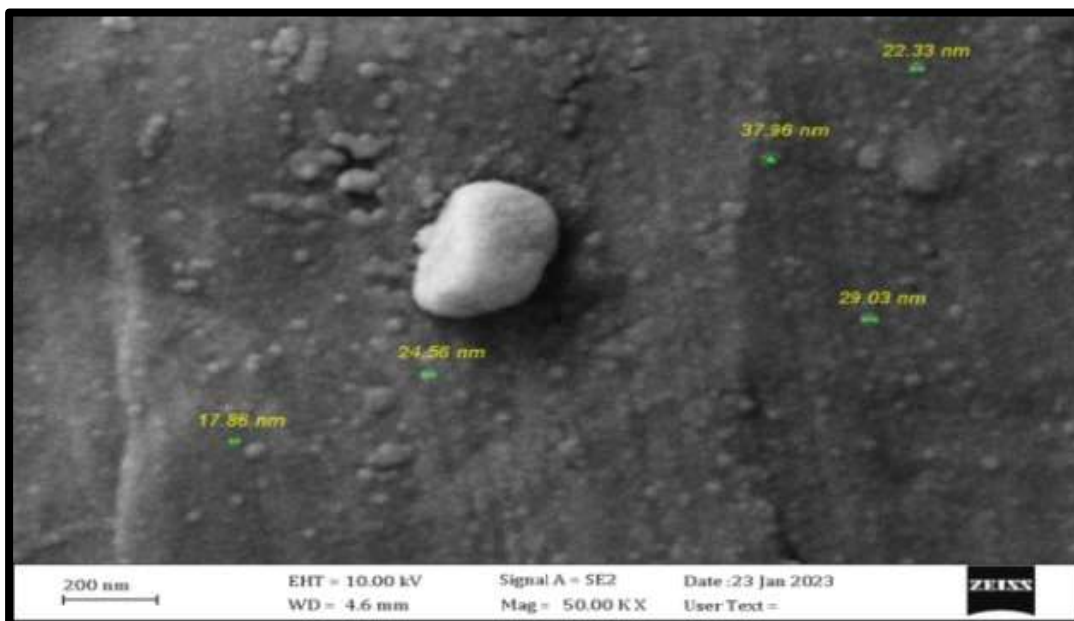
Figure (3) shows (FESEM) pictures showing the distribution of diameters (nm) of silver nanoparticles with the number of pulses (550,650, 800) pulses and the energy of 610 mJ, where we note that particles were obtained within the nanoscale range between (23.17 nm-65.65nm). Average size of diameters is (39.1 nm) and almost spherical.

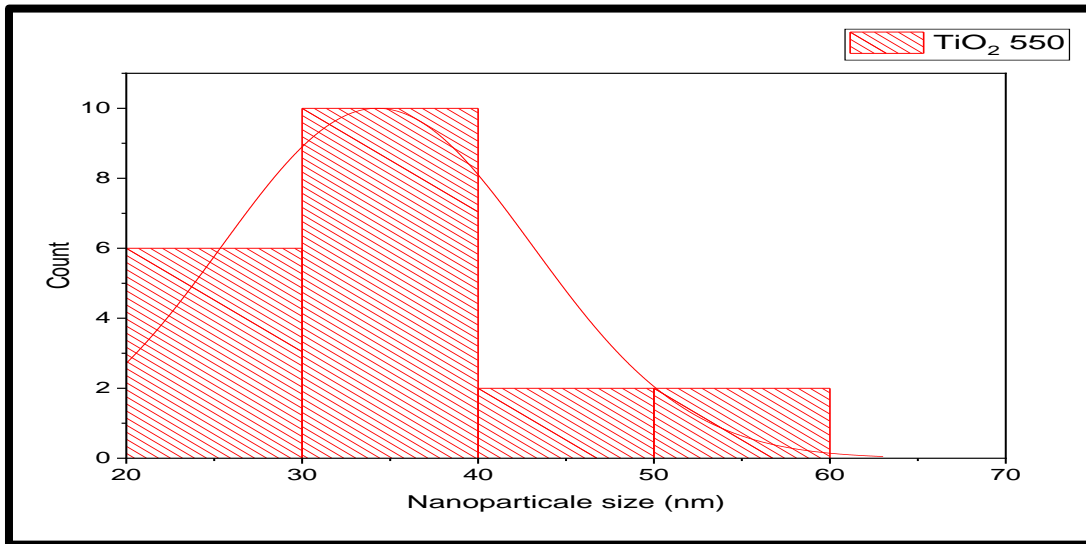




Figures 3: FE-SEM image of a Silver Nanoparticle (pulse 550) and Histogram and Kaosi diagram

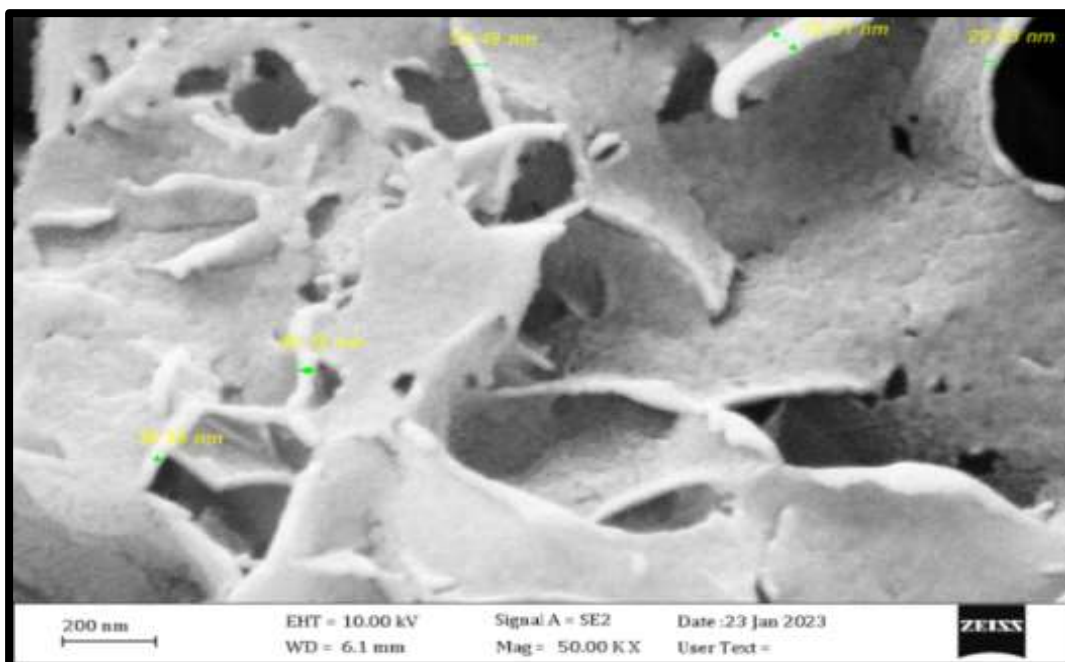
Figure (4) shows (FE-SEM) pictures showing the distribution of diameters (nm) of the Titanium Oxide nanoparticles by the numeral of pulse (550) pulses and, the vitality of 610 mJ, where we note that particles were obtained within the nanoscale range between (22.79 nm – 59.33 nm) Average size of diameters is (34.26 nm) and almost spherical.





Figures 4: FE-SEM image of a Titanium Oxide Nanoparticle (550) and Histogram and Kaosi diagram

Figure (5) shows (FE-SEM) pictures showing the distribution of diameters (nm) of Zinc Oxide nanoparticles by the quantity of pulse (550) pulses and, the energy of 610 mJ, where we note that particles were obtained within the nanoscale range between (17.79 nm -75.36 nm).Average size of diameters is(36.54nm)and almost spherical.



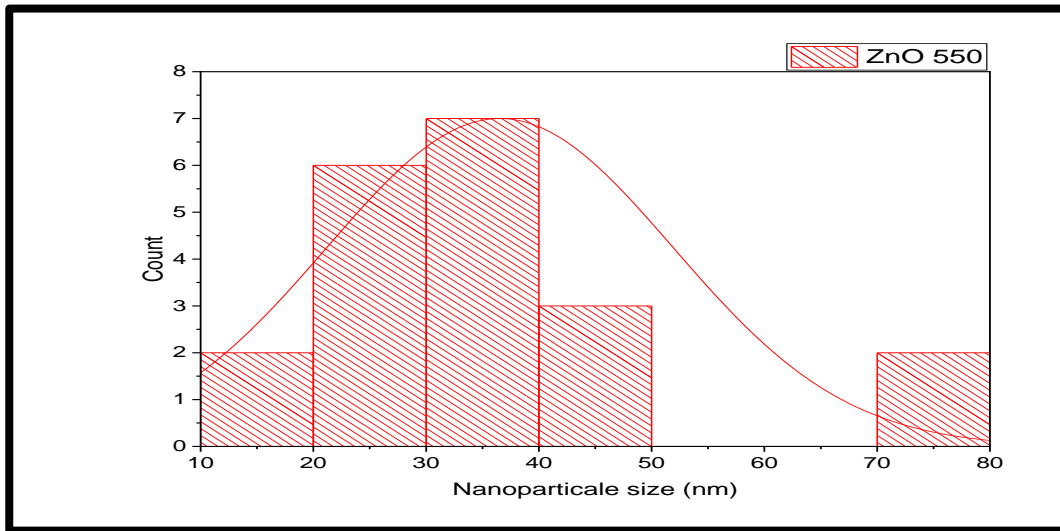
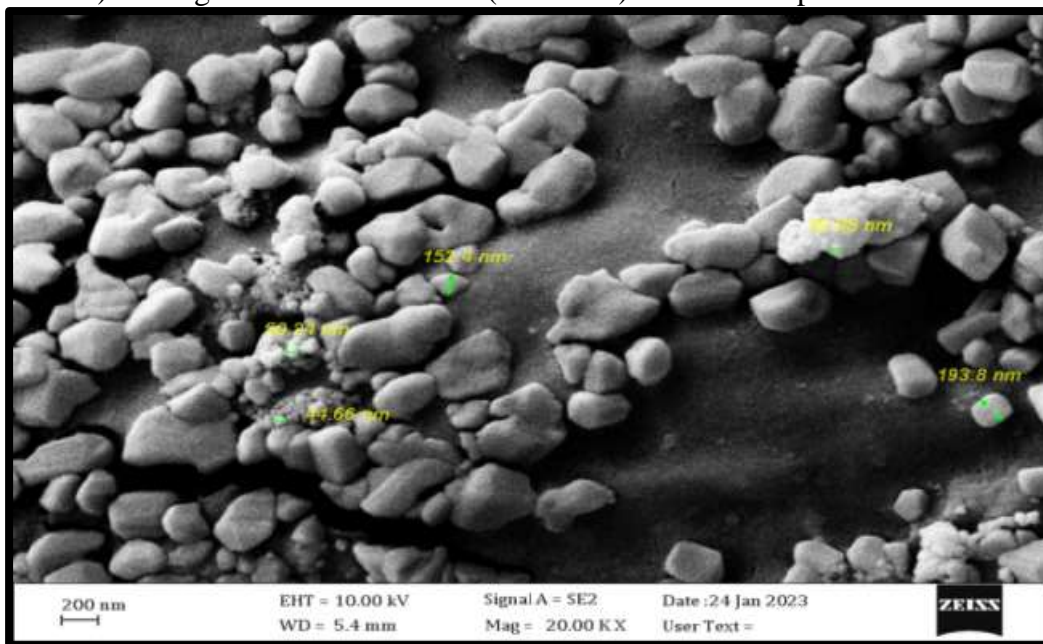
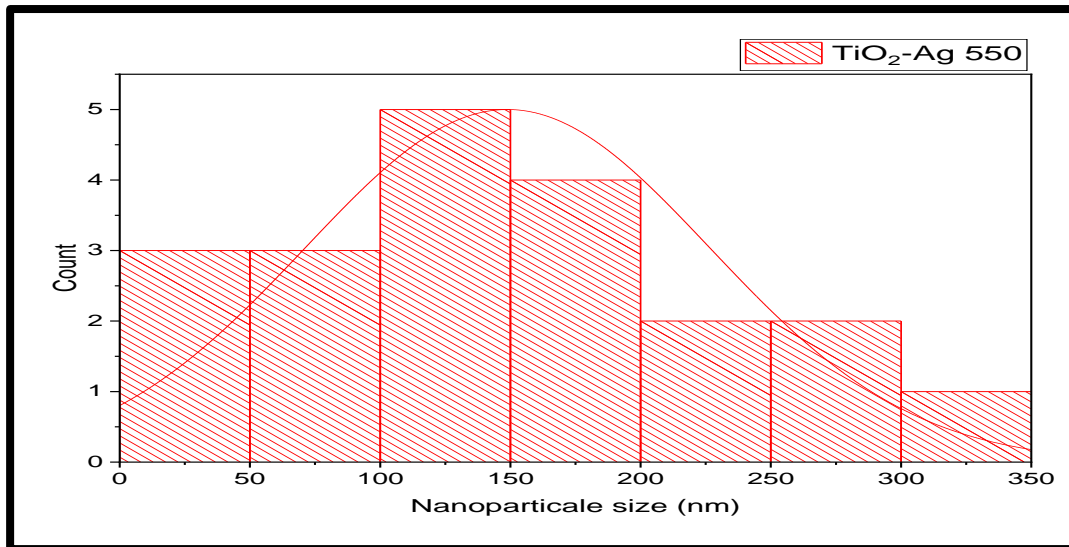


Figure 5: FE-SEM image of a Zinc Oxide Nanoparticle (550) and Histogram and Kaosi diagram

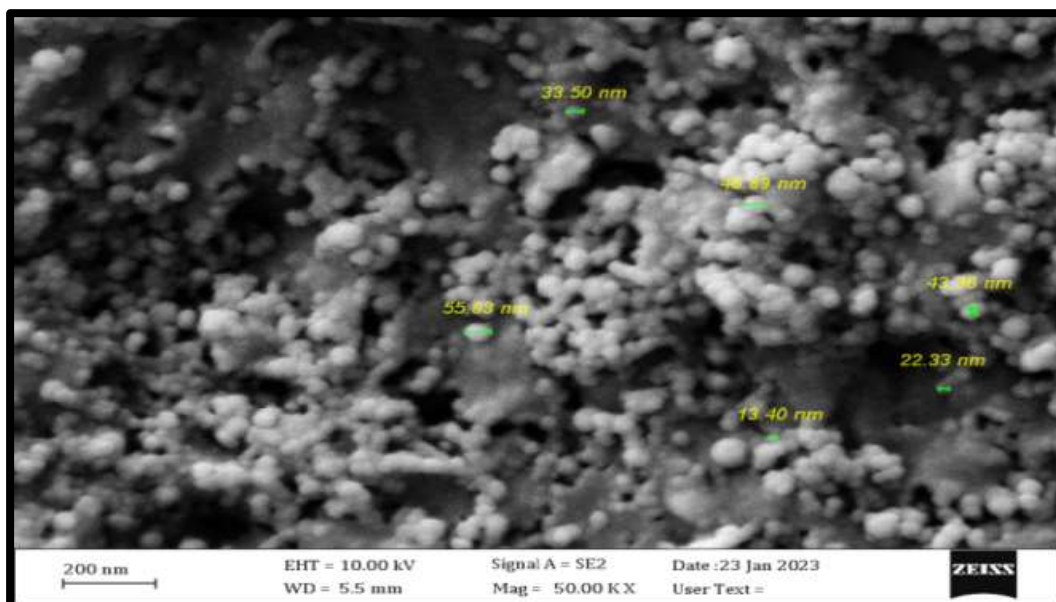
Figure (6) shows (FE-SEM) pictures showing the distribution of diameters (nm) of the TiO₂-Ag (550) nanoparticles with the quantity of pulses (550) pulses and the energies of 610 mJ, where we note that particles were obtained within the nanoscale range between (44.17 nm-307.39 nm) Average size of diameters is (172.2 nm) and almost spherical.

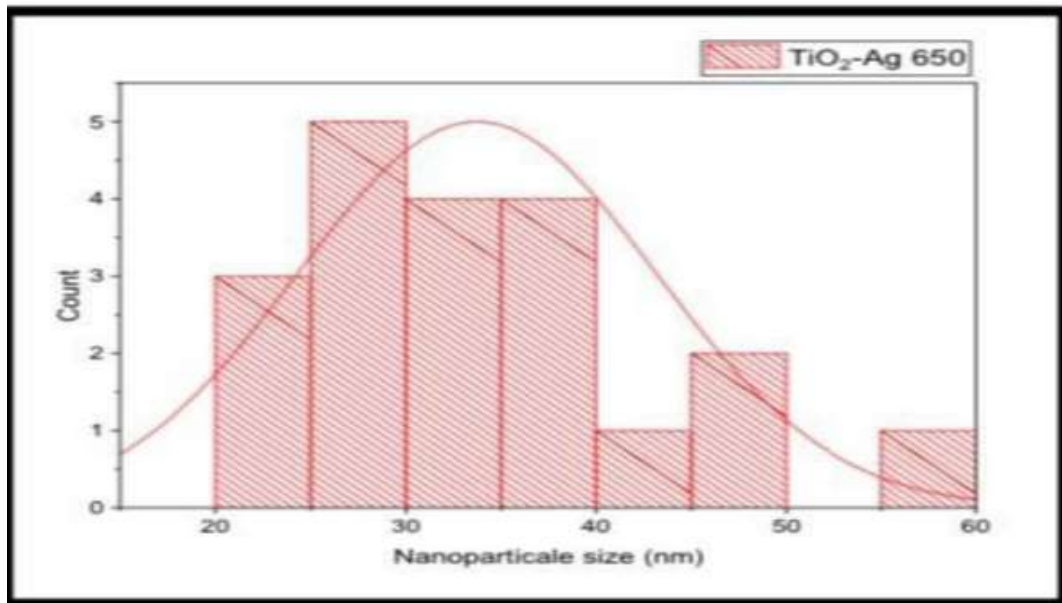




Figures 6: FE-SEM image of a $\text{TiO}_2\text{-Ag}$ (550) Nanoparticle and Histogram and Kaosi diagram

Figure (7) shows (FE-SEM) pictures showing the distribution of diameters (nm) of the $\text{TiO}_2\text{-Ag}$ (650) nanoparticles by the number of pulses (650) pulses then the energy is 610 mJ, where we note the particles were obtained within the nanoscale range between (20.48 nm -56.09 nm) Average size of diameters is (33.73 nm) and almost spherical.





Figures 7: FE-SEM image of a TiO₂-Ag-ZnO (550) Nanoparticle and Histogram and Kaosi diagram.

Results of Fourier Transform Infrared FTIR test

Figure (8) shows the infrared spectrum of (Ag, TiO₂, ZnO, Ag-TiO₂, Ag-TiO₂-ZnONPs) prepared in distilled water medium with pulse numbers (800) pulses and a constant ablation energy (610 mJ). Figure (8-a) as they are composed of distinct functional groups of pure (AgNPs) with the locations and intensity of the absorption bonds of (AgNPs), we note that the absorption bond appearing near the wave number (468.77 cm⁻¹) is due to the vibration of the (Ag-O) bond, and the absorption one appearing near the wave number (1641 cm⁻¹) is due to the vibration of the (H-O) group [8].

The broad peak at 3100–3600 cm⁻¹ is allocated to the fundamental stretching vibration of hydroxyl group (free or bonded), Ti-OH in our study. A weak band at 1624 cm⁻¹ is related to the bending vibration of coordinated H₂O, as well as Ti-OH. The broad band below 1000 cm⁻¹ (include minima at 754, 583, 522 and 471) cm⁻¹ can be ascribed to characteristic Ti–O and Ti–O–Ti stretching and bending vibrational modes for rutile TiO₂ sites, chemical compound connections, and bond sites for titanium dioxide. Note that the absorption beam appearing



near the wave number (443.77 cm^{-1}) is due to the (Ti-O) vibration and peaks between 900 and 850 cm^{-1} resemble the formation of O-Ti-O bonds [9].

Besides, the bands at region of 2887 cm^{-1} plus 2347 cm^{-1} represented the symmetric as well as anti-symmetrical vibrations mode which attribute to the presence of surfactant. A widespread absorbing bands witnessed within 450 to 850 cm^{-1} ranging showed Ti-O bending mode of vibrations that improves the creation of metallic oxygen bond.

In addition, presence peak at 800 cm^{-1} in state of Ag-TiO₂ nanocomposite while there is no peak in pure TiO₂ due to the Ti-O-Ag stretching vibrations of nanocomposite. Moreover, the results of FTIR spectrum reveal the increasing concentrations for O-H bands of Ag-TiO₂ nanocomposite because of the increasing of Ag content and lead to possible interaction of TiO₂ with Ag species.[10] and shows peaks at ($687.72, 738\text{ cm}^{-1}$) which is attributed to the formation of Zn-O bond, and absorption peaks around 3400 cm^{-1} and 1155 cm^{-1} are attributed to O-H stretching vibration of H₂O in ZnO and composite particles which may be caused by moisture absorption.

A sharp peak around 1600 cm^{-1} is attributed to H-O-H bending vibration, which is assigned to a small amount of H₂O in ZnO crystals. The medium weak band at 882 cm^{-1} is assigned to the vibrational frequency due to the Zn-O lattice. The significant decrease in intensity as well as slightly shifting towards higher value of the peak at 882 cm^{-1} in composite TiO₂-ZnO particle with compared to pristine ZnO revealed that chemically bonded TiO₂-ZnO composite was formed.

The intensity of peaks at $3400, 1600,$ and 892 cm^{-1} shifted towards lower value after loading Ag NPs on composite, the shifted peak of ZnO at (882 cm^{-1}) towards higher value when TiO₂ was loaded to ZnO, was found to be significantly shifted towards lower value after Ag loading Figure which revealed the deposition of Ag as well as formation of metal binary semiconductor composite. Ag atom is far heavier than Zn atom, therefore according to the well-established theories of irrational modes in mixed crystals the substitution should result in a downward shift of the fundamental transverse optical phonon mode [11].

Table 1: Shows chemical bonds by FTIR of Ag NPs, TiO₂ NPs, ZnO NPs, Ag-TiO₂ NPs, Ag-TiO₂-ZnO NPs.

X (cm-1)	Bonds
468.77	Ag-O
1641	C-O
443.77, 484.13	Ti-O
3450	O-H
890	O-Ti-O
650	Zn-O

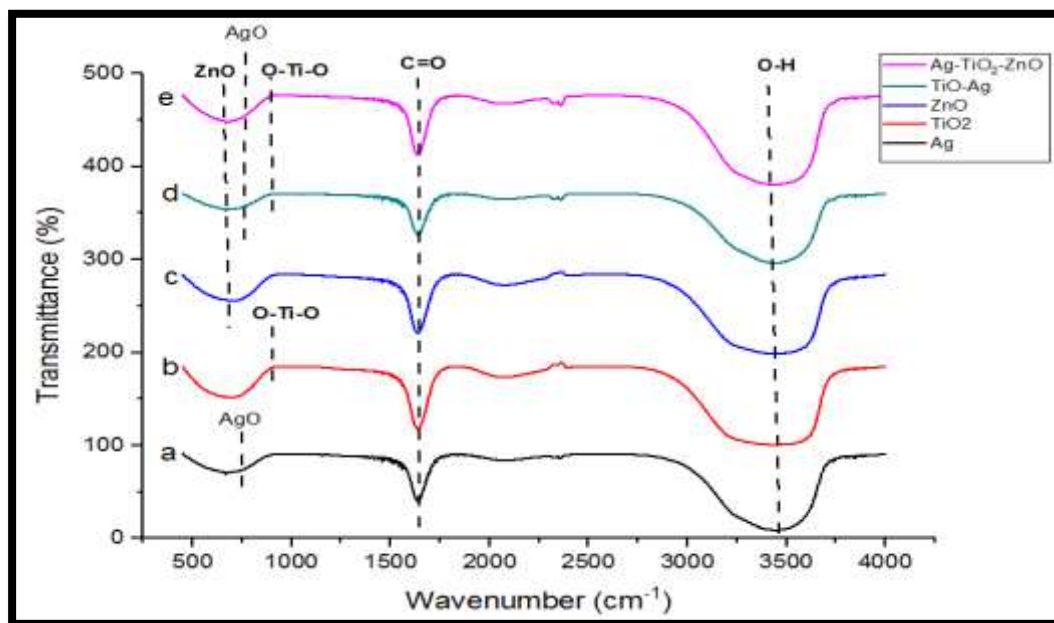


Figure 8: Fourier transforms of the infrared spectrum of a solution of Ag, TiO₂, ZnO, TiO₂-Ag and TiO₂-Ag-ZnO NPs.

Optical Properties

Effects of Laser Shots on Absorbency and Surface Plasmon Resonance

Titanium and silver nanoparticles were generated in colloidal solutions using pulsed laser liquid ablation (PLAL) technology. This was done to study the relationship between laser pulses and the size and properties of the nanoparticles. This article specifically studies the application of 610 mJ and pulse energies 550, 650 and 800. When a laser with a wavelength of 1064 nm is immersed in distilled water, it creates a spark column on the metal surface and shock waves propagate throughout the liquid.



The color and intensity of the solution changed with an increase in laser pulses, indicating the presence of metal nanoparticles in the extracted metal. Particularly in the UV-visible range, its SPR peaks confirmed the formation of titanium dioxide and silver nanoparticles [12]. The vibration and aggregation of electrons on the surface of the nanoparticle, along with an increase in the quantity and size of excised particles, are the causes of this alteration. As the number of pulses increases, the absorption intensity also increases.

The optical and ultraviolet emission spectra results for silver, titanium dioxide, and mixed colloidal solutions are shown in Figures (8), (9), and (10). Table (1) shows the absorption intensity and surface Plasmon resonance (SPR) spectrum results. Absorption spectroscopy studies showed changes in both the visible spectrum of silver and the ultraviolet region of titanium dioxide solutions. As the amount of laser pulse increases, the absorption intensity and SPR peak intensity also increase, resulting in different widths and heights of the absorption peaks.

Laser irradiation causes a spectral change indicating an increase in the number of nanoparticles, which is detected by the presence of a plasmon peak. This suggests that the nanoparticles are approximately spherical [12]

As can be seen in table (2) on figure (9), the position of the plasmon peak around (412nm) indicates the almost spherical form of the nanoparticles. This discovery is emphasized by the silver nanoparticles solution's absorption spectra [13].

Now picture this- 550, 650, even up to 800 pulses show themselves in our produced samples' absorption spectrum! We're talking silver nanoscale solution here.

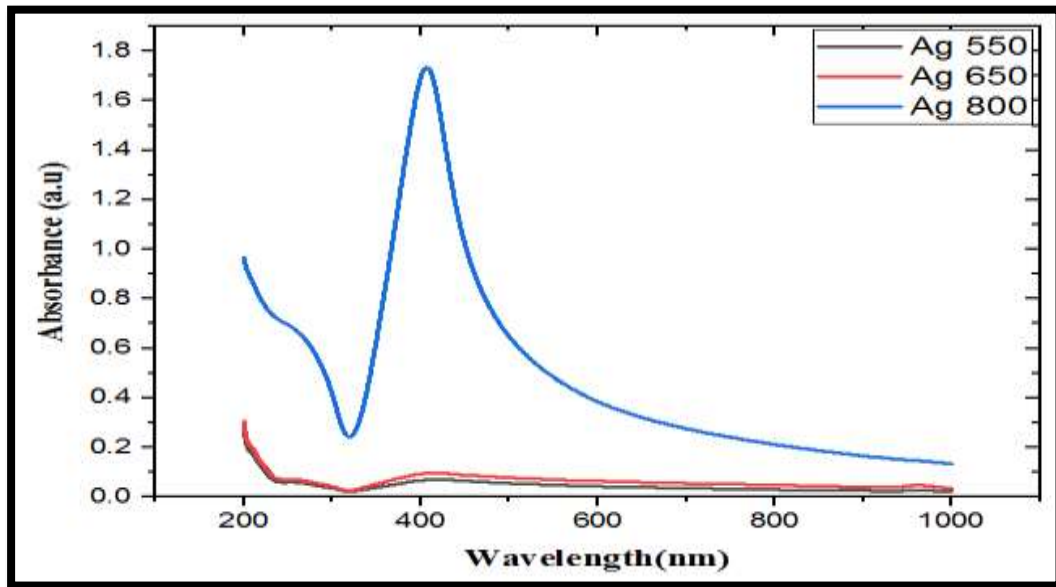


Figure 9: The Absorbance for the silver nanoparticle solution.

By the Figure (10), we note that Surface Plasmon resonance (SPR) peaks obtained for colloidal solution of nanoparticles of titanium dioxide. An increase in optical absorption was observed due to an increase in the formation of nanoparticles with an increase in the number of pulses and that they had a high absorption at short wavelengths (UV spectrum). Through this investigation, it was discovered that the material expelled from the target by the resultant particles, the titanium dioxide particles of the manufactured sample, had surface plasmon resonance peak locations at (291, 293, and 292) nm, as indicated in Table (2). Continues to exist in the liquid surrounding the target, creating a substance known as a colloidal solution. These particles have the ability to absorb laser energy and lessen the laser light's incident intensity. Because target removal effectiveness is influenced by three factors changes in solution polarity, higher diffusion as a result of high nanoparticle concentrations, and surface defects a drop is anticipated. The occurrence of the phenomenon of aggregation of the nanoparticles may lead to a change in the color of the suspension depending on the degree of aggregation of the particles [14-16].

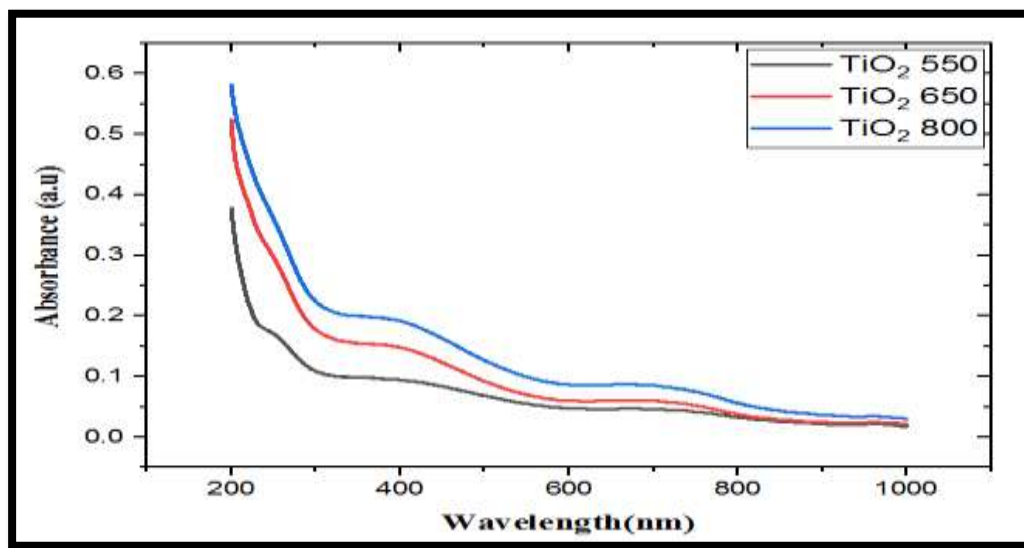


Figure 10: The Absorbance for the titanium dioxide nanoparticle solution.

It is possible to effectively observe the optical characteristics of quant size-produced nanoparticles using UV/VIS absorbance spectroscopy. Figure (11) shows the generated nanoparticles' spectrum of absorption for each of the three pulse energy values. The absorption spectra show that for the pulse energies (550, 650, and 800 mj), respectively, the peaks are located is (210, 211, and 213 nm).

This shows that zinc oxide nanoparticles are being produced within the fluid. As the pulse energy decreases, the solution's Plasmon band shifts (blue shifts) towards smaller wavelengths, revealing the production of additional nanoparticles. A shift in wavelength toward shorter ones indicates the creation of smaller nanoparticles as a result of the quantum confinement effect. The amount that is absorbed of the generated nanoparticles determines the absorption values; a higher concentration yields a larger absorption peak.

The outcomes indicate a greater absorption. Because of the larger concentration of generated nanoparticles in the solution, the consequences indicate a greater absorption peak amplitude for inordinate pulse dynamism. Table 1 explains how (UV/VIS) absorption assessment for 3 materials yields information about the impact from pulse vitality variation happening the absorption heights. As seen, the absorbed peaks change further towards the blue with increasing laser pulse energy, indicating the production of smaller nanoparticle sizes. [17].

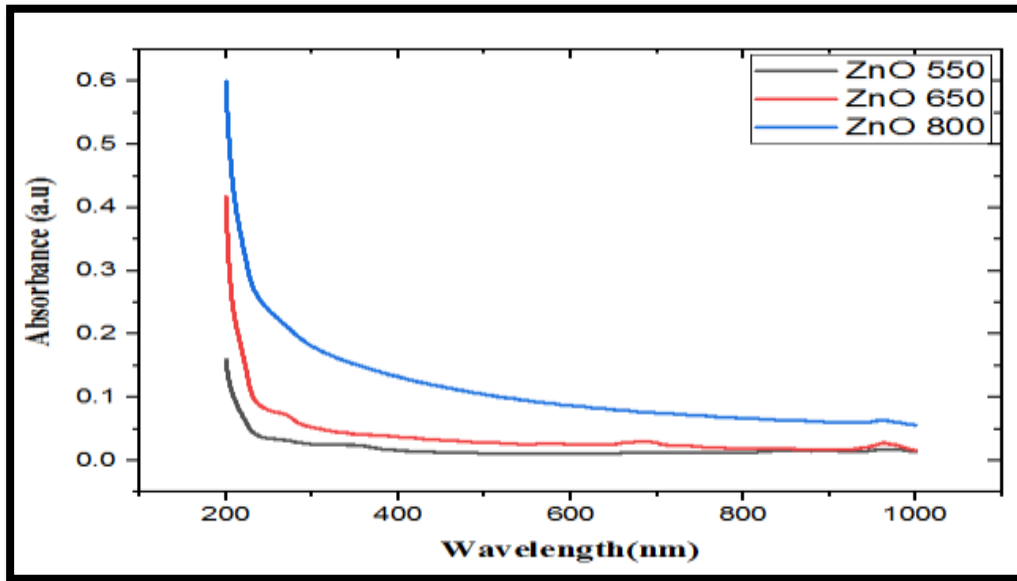


Figure 11: The Absorbance for the Zinc nanoparticle solution.

Figure (12) displays the spectrum of absorption the hybrid nanoparticles solution for Ag and TiO₂ nanoparticles and, we note presence of two plasmon peak positions for each as shown in Table (2), where we noticed that the locations of the SPR peaks of hybrid nanoparticle were fixed. Approximately (291) nm at the first site. We also observed that the peaks' positions in the second location of the hybrid nanoparticles were (from 407-410, 399-406 and 413-420) nm [18].

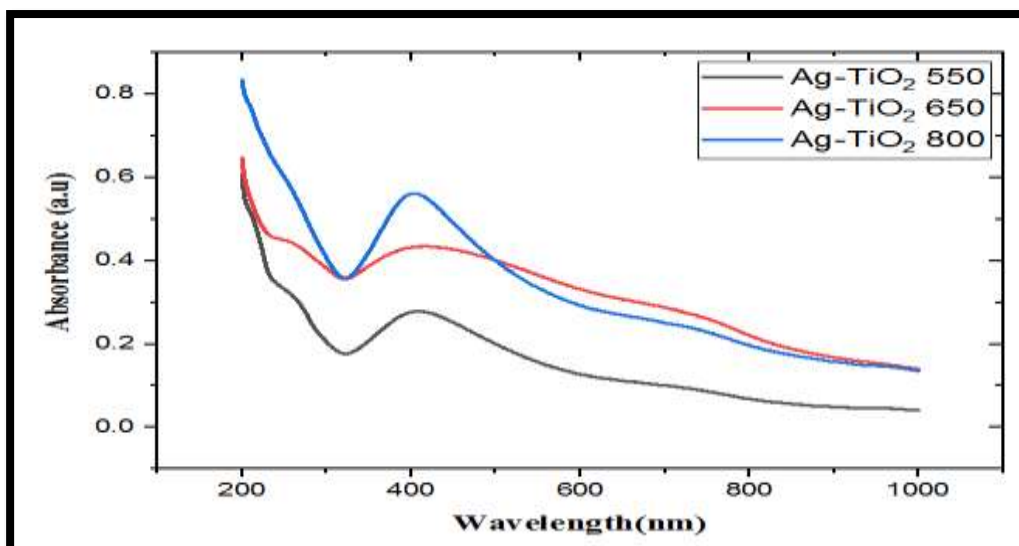


Figure 12: Absorption of TiO₂-Ag solution at a constant temperature.

Figure (13) shows the spectrum of absorption hybrid nanoparticle solutions containing TiO₂, silver nanoparticle and Zinc oxide. It is observed that each hybrid nanoparticle has two plasmon peak positions, as indicated in Table (4-3), indicating that the hybrid nanoparticles' surface plasmon resonance peak locations are fixed. At the first location, around (299.4-200.9) nm. We also observed that the peaks' positions in the second location of the hybrid nanoparticles were (412-420, 413-417 and 403-411 nm) [19].

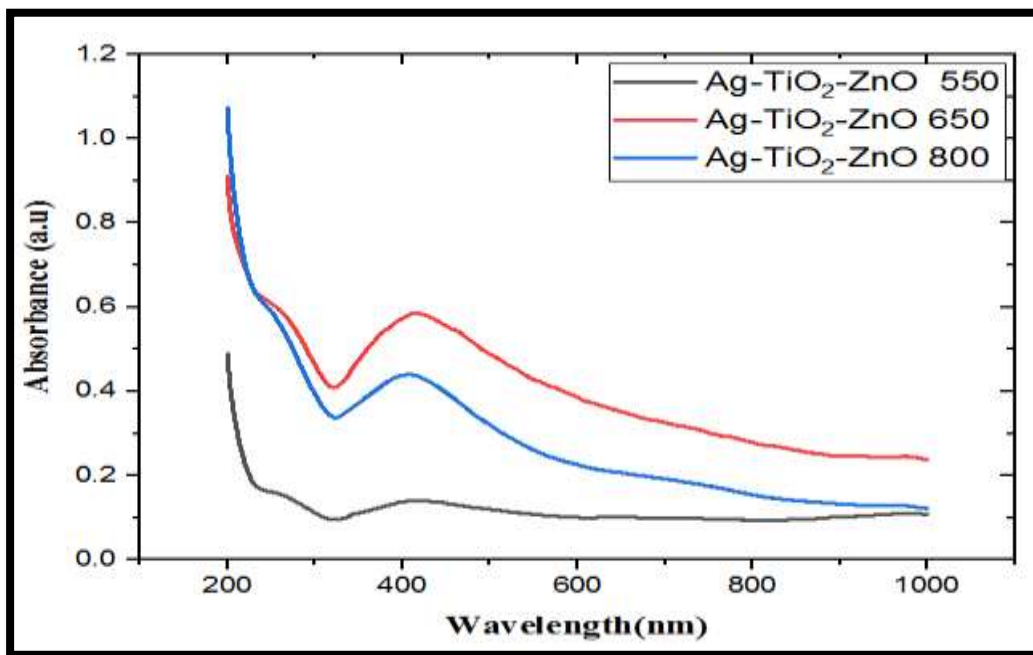


Figure 13: The nanoparticle solution of Ag-TiO₂-ZnO NPs absorption spectrum.



Table 2: The results of (SPR) and the intensity of absorption that we obtained from the absorbance spectrum at the wavelength (1064) nm, energy (610) mJ and the number of different pulses.

Nanoparticles in distilled water	Pulses Number	Energy (mJ)	Abs(a.u) Absorbency		Peak (nm) (SPR)	
Ag	550	610	0.27	199.9	0.07	411.9
	650	610	0.3	199.9	0.1	414
	800	610	0.96	199	1.73	406.6
TiO ₂	550	610	0.37		200	
	650	610	0.52		200	
	800	610	0.57		199.8	
ZnO	550	610	0.16		200	
	650	610	0.41		199.9	
	800	610	0.59		199.9	
TiO ₂ -Ag	550	610	0.6	199.9	0.28	407-410
	650	610	0.64	199.9	0.44	413-420
	800	610	0.83	200	0.56	399-406
TiO ₂ -Ag-ZnO	550	610	0.48	200.9	0.14	412-420
	650	610	0.91	199.4	0.58	413-417
	800	610	1.07	200	0.44	403-411

Conclusion

In this work, The Dioxide Titanium (TiO₂) , Silver (Ag) , Zinc Oxid (ZnO), hybrid Dioxide Titanium / Silver (TiO₂/Ag) nanoparticles and hybrid Dioxide Titanium / Silver/Zinc Oxide (TiO₂/Ag/ZnO) nanoparticles were prepared using laser pulse ablation by surface Plasmon resonance. Ablation was performed at a wavelength of 1064 nm under ideal experimental conditions, with pulses (550, 650, 800) and a constant energy of 610 mJ.

This study was conducted by studying the optical and structural properties of and titanium dioxide / silver nanoparticles and enhaneing the optical properties through the hybrid compound. Analyzes confirmed by UV-visible, FE-SEM, FTIR, and antibacterial, (FE-SEM) results showed that we could obtain almost spherical nanoparticles.

As for the optical properties of the hybrid, the UV results indicated a distinctive peak with suitable wavelengths.

Bare and hybrid nanoparticles compound have been used in the biological application to inhibit bacterial species, and four types of bacteria have already been inactivated. It can be



concluded that work merges nanotechnology and bacteriology leading to new long-lasting bactericides.

Source of funding: The source of funding is self-funding

Conflict of interest: There is no conflict of interest for authors

References

- [1] Y. Herbani, R. S. Nasution, F. Mujtahid, S. Masse, Pulse laser ablation of Au, Ag, and Cu metal targets in liquid for nanoparticle production, In Journal of Physics: Conference Series 985(1), 012005(2018), DOI([10.1088/1742-6596/985/1/012005](https://doi.org/10.1088/1742-6596/985/1/012005))
- [2] N. M. Jassim, K. Wang, X. Han, H. Long, B. Wang, P. Lu, Plasmon assisted enhanced second-harmonic generation in single hybrid Au/ZnS nanowires, Optical materials, 64, 257-261(2017), DOI([10.1016/j.optmat.2016.11.034](https://doi.org/10.1016/j.optmat.2016.11.034))
- [3] Y. Wang, H., Chen, S. Dong, Dong, E. Wang, Surface-enhanced Raman scattering of silver-gold bimetallic nanostructures with hollow interiors, The Journal of chemical physics, 125(4), (2006), DOI(<https://doi.org/10.1063/1.2216694>)
- [4] R. K. Ismail, R. Al-Haddad, T. H. Mubarak, Time effect on the red shift of surface plasmonic resonance core-shell SiO₂: Gold nanoparticles (AuNPs), In: AIP Conference Proceedings, 2190(1), (2019), DOI([10.1063/1.5138581](https://doi.org/10.1063/1.5138581))
- [5] J. A. Scholl, A. L. Koh, and J. A. Dionne, Quantum Plasmon Resonances of Individual Metallic Nanoparticles, Nature, 483 (7390), 421-427 (2012), DOI([10.1038/nature10904](https://doi.org/10.1038/nature10904))
- [6] M. Rycenga, C. M. Cobley, J. Zeng, W. Li, C. H. Moran, Q. Zhang, D. Qin, and Y. Xia, Controlling the Synthesis and Assembly of Silver nanostructures for Plasmonic Applications, Chemical Reviews, 111(6), 3669-3712(2011), DOI(<https://doi.org/10.1021/cr100275d>)
- [7] Q. A. Guidan, T. H. Mubarak, N. M. Jassim, Preparation of Aluminum nanoparticles by pulsed laser ablation and its use in reducing Iron Corrosion, Journal of Optoelectronics Laser, (2022)



- [8] R. Ponnusamy, D. Sivasubramanian, P. Sreekanth, V. Gandhiraj, R. Philip, G. Bhalerao, M. H. Sabbar, Synthesis and Characterizations of Nano Magnetic Particles (Co-Ni Fe₂O₄) Ferrite by Co-precipitation and Biomedical Application, International Journal of Nanoelectronics and Materials, 16, 135-144(2023), DOI(<https://doi.org/10.24996/ijns.2020.61.2.12>)
- [9] T. H. Mubarak, N. M. Jassim, Q. A. Guidan, Some physical properties of Al nanoparticle Via pulse laser ablation in liquid method (PLAL), Academic Science Journal, 1(2), 66-81
- [10] C. L. Sajti, R. Sattari, B. N. Chichkov, and S. Barcikowski, Gram scale synthesis of pure ceramic nanoparticles by laser ablation in liquid, The Journal of Physical Chemistry , C114(6) , 2421-2427(2010), DOI([10.3461/bjnano.6.191](https://doi.org/10.3461/bjnano.6.191))
- [11] N. M. Jassim, Synthesis and nonlinear optical responses of Ag: ZnO core: shell nanoparticles induced by Z-scan technique, J Opt (2024), DOI(<https://doi.org/10.1007/s12596-024-02432-6>)
- [12] M. Rai, A. Yadav, and A. Gade, Silver nanoparticles as a new generation of antimicrobials, Biotechnol Adv, 27, 76-83 (2009), DOI([10.1016/j.biotechadv.2008.09.002](https://doi.org/10.1016/j.biotechadv.2008.09.002))
- [13] M. E. Vance, T. Kuiken, E. P. Vejerano, S. P. McGinnis, M. F. Hochella, D. Jr. Rejeski, M. S. Hull, Nanotechnology in the real world: Redeveloping the nanomaterial consumer products inventory, Beilstein J. Nanotechnol, 6, 1769–1780(2015), DOI([10.3762/bjnano.6.181](https://doi.org/10.3762/bjnano.6.181))
- [14] K. Oura, V. G. Lifshits, A. A. Saranin, A. V. Zotov, and M. Katayama, Surface science: an introduction, Springer Science and Business Media, (2013), DOI([10.1017/j.biotechadv.2008.00.012](https://doi.org/10.1017/j.biotechadv.2008.00.012))
- [15] N. M. Jassim, Femtosecond Optical Nonlinearity Signal and Dark Field Scattering Microscopy of Gold Coated Zinc Oxide Nanowires, NeuroQuantology: An Interdisciplinary Journal of Neuroscience and Quantum Physics, 18(8), (2020)



- [16] M. Lau, B. Gökce, G. Marzun, C. Rehbock, and S. Barcikowski, Rapid nanointegration with laser-generated nanoparticles, (2015), DOI([10.1016/j.biotechadv.2009.08.202](https://doi.org/10.1016/j.biotechadv.2009.08.202))
- [17] N. M. Jassim, N. I. Ibrahim, N. Z. Khalaf, Z-scan Study of the Non-linear Optical Properties of Silver/Curcumin Dye Nanocomposites Prepared Via Nanosecond Pulsed Laser Ablation, *Revue des Composites et des Materiaux Avances*, 34 (4), 533-540(2024), DOI(<https://doi.org/10.18280/rcma.340415>)
- [18] A. Z. Marid, and Q. Adnan, Influence of Magnetic Field on Silver Nanoparticles Synthesized by Laser Ablation, *Iraqi Journal of Science*, 341-350(2020), DOI(<https://doi.org/10.24996/ijs.2020.61.2.12>)
- [19] N. Kareem, N. I. Ibrahim, B. A. M. Sumayyah, Investigation on synthesis, structural and nonlinear optical responses of cadmium selenide coated with gold nanoparticles induced by femtosecond laser excitation, *Eastern-European Journal of Enterprise Technologies*, 3 (5 (111), 13–18(2021), DOI(<https://doi.org/10.15587/1729-4061.2021.231422>)